DOI: 10.13009/EUCASS2022-6123
9TH EUROPEAN CONFERENCE FOR AERONAUTICS AND SPACE SCIENCES (EUCASS)

Implementation Aspects of Uniform Blowing in Turbulent Boundary Layers

Georg Fahland, Davide Gatti, Alexander Stroh
and Bettina Frohnapfel
Institute of Fluid Mechanics, Karlsruhe Institute of Technology,
Kaiserstr. 10, 76131 Karlsruhe, Germany
georg.fahland@kit.edu

Abstract

We investigate the active turbulent boundary layer control (BLC) scheme of uniform blowing also known as micro-blowing technique applied on airfoils. In this contribution we will show the path relating numerical investigations to experimental investigations which we are currently preparing. A significant effort was put in understanding the differences previous experimental campaigns showed compared to numerical results. Therefore, we conduct a theoretical analysis of the momentum budget including the fluid utilized for control application. From this we draw a conclusion for the inevitable drag contribution of this control scheme as well as understanding the relation of different drag measurement techniques. We show the application of these findings for a zero pressure gradient turbulent boundary layer flow via Direct Numerical Simulation (DNS). Furthermore we apply a set of Reynolds-Averaged Navier-Stokes (RANS) simulations to show the impact of these findings for varied control parameters in order to demonstrate the significance of the findings for both the relation of measurement quantities as well as the inevitable drag contributions of the support system. With this we give an overview of the prepared experimental setup which we plan on using to validate some of the numerical results in terms of aerodynamic performance enhancement capabilities as well as demonstrate the validity of the concepts regarding the drag relations.

1 Introduction

Active flow control has been a continuous field of research in the last decades with the goal of performance enhancement, especially for mobile applications such as aircraft. It started with Prandtl proposing suction to prevent separation in adverse pressure gradient boundary layers [19, p. 42]. Applied to airfoils it was soon discovered that suction in order to prevent separation also has the beneficial effect of delaying the transition to a turbulent boundary layer [8]. This is still a very active field of research in order to significantly reduce fuel consumption on commercial aircraft [2, 20] with first adaptions by the industry on the Boing 787 tailplane [16]. However, preventing laminar-turbulent transition is very sensitive to changes in conditions which opens the field for turbulent boundary layer drag reduction control schemes if a turbulent boundary layer (TBL) cannot be avoided. Flight tests were done using the passive control scheme of riblets [24] but also active schemes were proposed, e.g. wall-parallel blowing in the aft region of an airfoil to control lift [23]. Also, this is still an active field of research [18] despite successful implementations on aircraft [17] already. The scheme of wall-normal uniform blowing aims at reducing the wall friction of a TBL directly. First efforts date back to the 1960s [13]. A major contribution to the field was done around the year 2000 by Hwang which is summarized in [9]. It was shown that significant friction reduction and thus performance enhancement by reduction of the drag of the body could be accomplished. In the following more numerical investigations were done [11, 12, 21, 1] to better understand the properties of a TBL subject to uniform blowing. Furthermore it was shown that the scheme of uniform blowing on the pressure side of an airfoil has a prospect of significant performance enhancement regarding the drag force on the airfoil itself [6]. The experimental implementation of uniform blowing is resembled the closest by the so-called micro-blowing technique. Experiments showed partially good agreement but also some considerable deviation to numerical results [5, 15, 14]. This raises two questions in order to understand if the performance enhancement which was shown numerically can be implemented in a real-world application similar to other control schemes mentioned above:

DOI: 10.13009/EUCASS2022-6123

- *What is the best way to resemble the uniformity assumed numerically using the micro-blowing technique?* This question focuses around the porosity $\phi_H = A_H/A$ which is a measure of the open area A_H in respect to the total area A of a surface.
- *What is the inevitable cost to provide the mass flux for such a control scheme in terms of system-related drag?* One aspect which got almost no attention so far is the momentum budget of the mass flux which is used for the control scheme. As we will show this is by far the most significant part which is also fundamental in the limits it puts to the overall performance enhancement possibilities.

In the methodology chapter we will show the numerical means of the investigations to answer the second question. We also show the momentum budget assessment which we will apply on the results in the following chapter. The discussion regarding the momentum budget reveals a fundamental difference for the measurement quantities in experiments. In the last chapter we will derive the implications for the design of our upcoming experimental campaign and show the general setup.

2 Methodology

2.1 Numerical Methods

In order to show the generality of our findings we process data of two previous publications: Direct Numerical Simulations (DNS) on zero pressure gradient (ZPG) turbulent boundary layers (TBL) were conducted by Stroh [21]. The data was reprocessed in order to find the necessary quantities for the von Karman equation (see equation 6). Secondly we conducted a series of Reynolds Averaged Navier-Stokes (RANS) simulations with the setup of Fahland *et al*. [6]. In order to assess the relations of different drag components (see section 2.2) we sampled the necessary values in the wake of the airfoil to evaluate the formula of Betz [3] in order to assess the drag of the airfoil.

2.2 Momentum Budget of support system

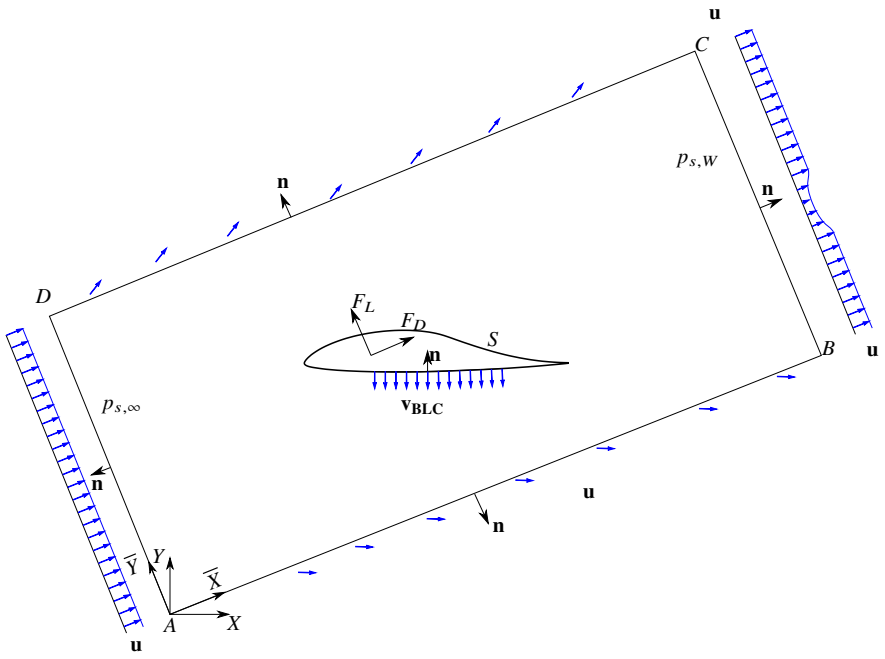

Figure 1: Control Volume (CV) for the airfoil momentum budget in which **n** is the normal vector pointing out of the CV).

In order to assess the momentum budget of a system with uniform blowing control scheme one can look at the problem from a measurement point of view – one way to determine the drag of a body is the integral force measurement of this body. We term this the *body drag* which we present as the dimensionless drag coefficient $c_{d,B}$. It represents the drag force F_D, acting in the free stream direction $\overline{\mathbf{X}}$ (see figure 1), normalized by the free-stream

DOI: 10.13009/EUCASS2022-6123

total pressure $q_\infty = \rho/2U_\infty^2$ and a reference area $S_{ref} = s \cdot c$ with span s and chord c:

$$c_{d,B} = \frac{2F_D}{\rho U_\infty^2 S_{ref}} = \frac{2}{\rho U_\infty^2 S_{ref}} \left(\iint_S p\mathbf{n} + \tau\mathbf{t} \quad dS \right) \cdot \overline{\mathbf{X}}, \tag{1}$$

where $\mathbf{n}$ and $\mathbf{t}$ correspond to normal and tangential unit vectors in respect to the surface. Integrating across the whole control volume perimeter which is put around the body (see figure 1, $\overline{ABCD}$) will also result in the body drag if the flux across the body surface is not taken into account separately.

The second possibility of drag estimation is to measure the momentum deficit downstream of the body (see figure 1, line $\overline{BC}$) in order to assess the drag which we call the *wake survey drag* $c_{d,W}$. Multiple wake survey methods are reported for application in practice, e.g. by Jones [10] and Betz [3]. These methods commonly result in a formulation linked to the momentum thickness of a boundary layer if the pressure behind the body has recovered to the free-stream static pressure:

$$c_{d,W} = \underbrace{\frac{2}{c} \int_B^C \frac{u}{U_\infty}\left(1 - \frac{u}{U_\infty}\right) d\overline{Y}}_{\text{momentum contribution}} + \underbrace{\frac{2}{c} \int_W -\frac{\overline{u'^2}}{U_\infty^2} d\overline{Y}}_{\text{Reynolds stress term}}. \tag{2}$$

Both considered methods by definition yield almost identical results for the drag coefficient of a 2D flow around a body. For the *wake survey drag* it is assumed that the flux leaving the control volume over the top ($\overline{CD}$) and bottom ($\overline{AB}$) edges has the free-stream velocity U_∞. Since this is not entirely true for a finite CV, this leads to minor deviations in the drag assessment compared to integrating over the whole CV surface or the body surface. These deviations can be addressed by introducing a correction factor which is constant for similar farfield solutions, *i.e.* minor boundary layer changes do not cause significant changes to the correction factor. This is also observed in our results.

However, in the case of an airfoil with additional mass flux through its surface like uniform blowing a correction term $c_{d,S}$ has to be introduced covering for the inflow-momentum introduced by the uniform blowing with the intensity v_{BLC} over the control region length l_{BLC}:

$$c_{d,B} = \underbrace{\underbrace{\int_B^C \underbrace{\frac{2}{c}\frac{u_{\overline{X}}}{U_\infty}\left(1 - \frac{u_{\overline{X}}}{U_\infty}\right)}_{f_{\text{def. U}}} d\overline{Y}}_{f_{\text{ReStress}}} + \int_B^C \underbrace{\frac{2}{c}\left(-\frac{\overline{u'^2}}{U_\infty^2} + \frac{\overline{v'^2}}{U_\infty^2}\right)}_{f_{\text{ReStress}}} d\overline{Y}}_{\text{wake survey drag } c_{d,W}} \underbrace{-2\frac{v_{BLC}}{U_\infty}\frac{l_{BLC}}{c}}_{\text{source thrust } c_{d,S}}. \tag{3}$$

Simplified this reads as

$$c_{d,B} = c_{d,W} \underbrace{-2\frac{v_{\text{BLC}}}{U_\infty}\frac{l_{\text{BLC}}}{c}}_{c_{d,S}}. \tag{4}$$

It will be shown that the thrust-like contribution of the correction term $c_{d,S}$ plays a significant role in the drag budget if the uncontrolled case is compared with the microblowing case. For the realization of blowing technique in a real world application the fluid expelled at the surface of the body has to be taken from somewhere else. If this source of fluid is ultimately the free-stream which the body is experiencing, then the momentum-loss drag $c_{d,ML}$ linked to the utilization of this fluid will be inevitably equal to the same term as the source thrust $c_{t,S}$ but with an opposite sign. This can be shown by applying the momentum budget to an isolated air-intake where the control fluid is drawn from the free-stream. Consequently we introduce the *inclusive drag* $c_{d,\text{inc.}}$ which accounts for this drag portion:

$$\underbrace{c_{d,\text{inc}}}_{\text{inclusive drag}} = \underbrace{c_{d,B}}_{\text{body drag}} + \underbrace{c_{d,ML}}_{\text{momentum loss drag = -}c_{d,S}} = \underbrace{c_{d,W}}_{\text{wake survey drag}}. \tag{5}$$

The *inclusive drag* includes the sink drag of taking in fluid from the free-stream and it is equal to the *wake survey drag*. In the case of an alternative source of fluid the *body drag* resembles the relevant drag for performance evaluation which is less then the *wake survey drag*.

Inspired by the similarity of this result with the formulation of the momentum thickness [19, p. 191] a more general approach on how a mass defect acts on the momentum balance can be motivated. The drag savings reported from the reduction of the friction velocity u_τ do not resemble the overall drag reduction if blowing is applied which is provided by the same free-stream it is supposed to reduce the drag with.

DOI: 10.13009/EUCASS2022-6123

Reassessing the von Karman equation we see the similarity of the momentum loss drag $c_{d,ML} = -c_{d,s}$ depicted above with the term associated to the wall-normal injection velocity v_{BLC}. This leads us to treat it as *supply loss coefficient* c_s for the localized boundary layer formulation in the von Karman equation:

$$\underbrace{c_{f,l} + \underbrace{2\frac{v_{\mathrm{BLC}}}{U_e}}_{\text{supply loss coefficient } c_s}}_{\text{inclusive loss coefficient } c_{\mathrm{inc}}} = 2\frac{\partial \delta_\theta}{\partial x} + 2\frac{2\delta_\theta + \delta^\star}{U_e}\frac{\partial U_e}{\partial x}. \tag{6}$$

Here U_e stands for the velocity at the edge of the boundary layer. In a zero pressure gradient boundary layer simulation this is identical to the velocity at infinity U_∞. In a more general case the the wall shear stress τ_w is normalized with the velocity at infinity rather than the local velocity at the edge of the boundary layer:

$$\underbrace{c_{f,\infty} + \underbrace{2\frac{v_{\mathrm{BLC}}U_e}{U_\infty^2}}_{\text{supply loss coefficient } c_s}}_{\text{inclusive loss coefficient } c_{\mathrm{inc}}} = 2\frac{U_e^2}{U_\infty^2}\frac{\partial \delta_\theta}{\partial \overline{x}} + 2U_e\frac{2\delta_\theta + \delta^\star}{U_\infty^2}\frac{\partial U_e}{\partial \overline{x}}. \tag{7}$$

with $\overline{x}$ being the wall parallel coordinate.

The force on the body is only given by the friction in case of the flat plate. In case of a provision of the BLC from free-stream the supply loss coefficient c_s equals the sink drag of a necessary intake of fluid. It has the same form of the sink drag of a whole body in equation 3, *i.e.* it is integrated over the length of the body in case of a plane flow. Therefore, the total drag is the sum of both the friction on the body and the supply losses.

The formula for both the integral drag forces as well as the boundary layer formulation show the necessity to have an accurate measurement of the local control scheme mass flux. This is not just important for labeling the measurement with the correct control intensity but also to get the correct relation of *body drag* to *inclusive drag*, especially if the measurement principle allows only for one of those values to be obtained directly.

3 Numerical Results

3.1 Boundary Layer

First we take a look at the local boundary layer momentum budget. The relation of *body drag* - which in a flat plate experiment consists solely of *friction drag* - and *inclusive drag* is present even if the origin of the BLC fluid is not investigated directly. Figure 2 shows the *inclusive drag* coefficient $c_{d,\mathrm{inc.}}$ derived from both the c_f calculated from the wall shear stress τ_w plus the correction term as well as the *inclusive drag* coefficient calculated from the control volume investigation. Despite neglecting the Reynolds stresses in the control volume analysis the agreement between them is clear. In fact, this is no surprise because it simply complies with the von Karman equation. The important part here is, that while the wall shear stress is indeed reduced by the control scheme of uniform blowing as reported multiple times [21, 11, 4, 9] the *inclusive drag* which is represented either by the left hand side or the right hand side of equation 6 is higher than the reference case. This means that including the provision of the control fluid the overall drag is increased by the flow control scheme although the wall shear stress is reduced. In order to avoid this unfavourable result one needs to use a source of control fluid where the momentum-wise effort of providing the control fluid has already been included. In such a case the reduction in wall shear stress is the relevant quantity for the drag estimate. Such conditions can be obtained e.g. by having a second flow control scheme which applies suction to the boundary layer and thus has left-over control fluid which can be used for the blowing control scheme.

DOI: 10.13009/EUCASS2022-6123

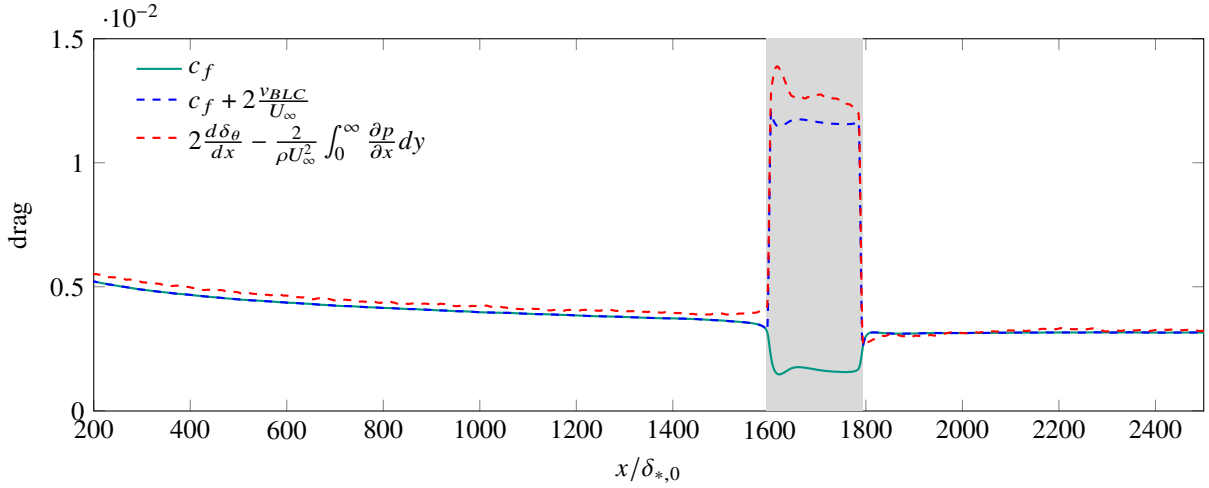

Figure 2: Evaluation of Eq. 6 for controlled TBL with $v_{BLC} = 0.005U_\infty$ placed at $x/\delta_{*,0} = 1594 - 1794$ (grey shading). Data adopted from [22].

3.2 Integral Drag forces

Similar to the localized formulation for the *inclusive drag* we motivated the quantity for integral drag estimates. The corresponding assessment can be found considering the wake profiles (figure 3). The figure shows the integrants of the wake integral to determine the *wake surve drag* and therefore the *inclusive drag* for the schemes blowing on the suction side (SS, figure 3 a)) and blowing on the pressure side (PS, figure 3 b)) of an airfoil.

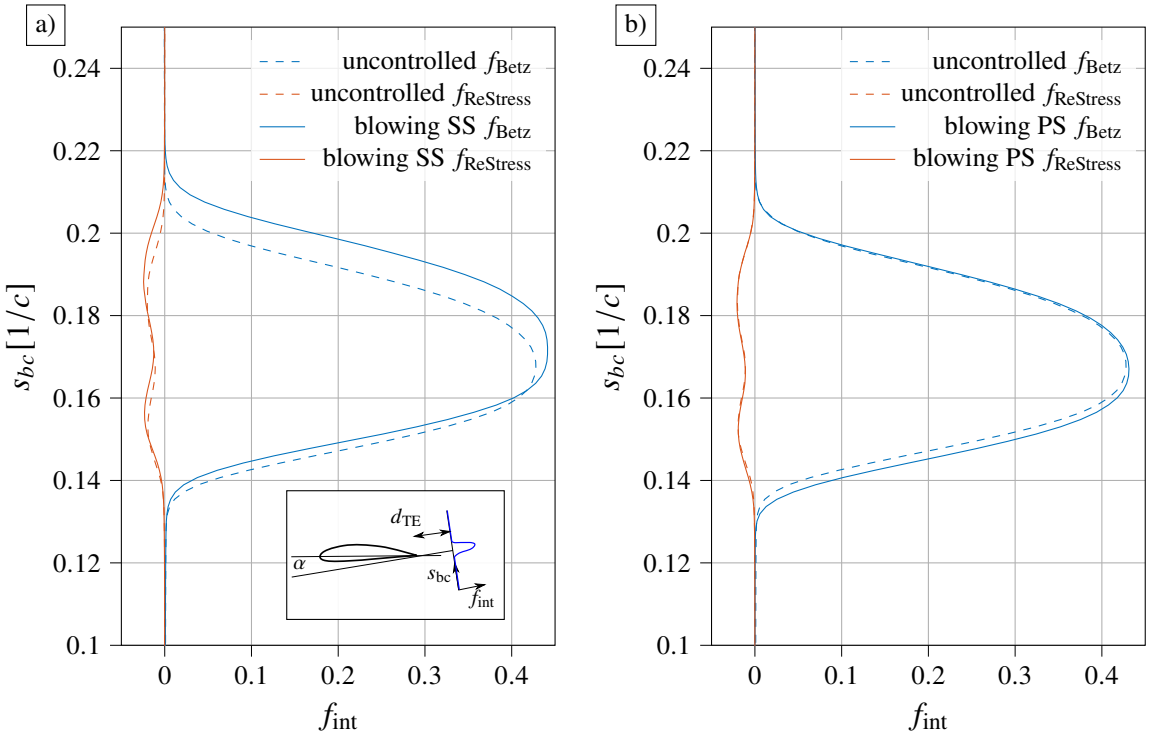

Figure 3: Wake profile integrant of Betz formula [3] and Re-Stresses (equation 3) for blowing on the SS and blowing on the PS at $d_{TE} = 0.2c$ behind trailing edge. NACA 4412, angle of attack $\alpha = 5°$, $Re = 4 \cdot 10^5$, $v_{\text{BLC}} = 0.1U_\infty$. LES data.

Clearly, for the blowing on the SS case one can see the significant increase in wake-size and therefore the associated increase of *inclusive drag*. The increase in the Re-Stress contribution, which acts negatively on the drag budget cannot mitigate the overall drag increase. Moreover it correctly indicates that the blowing on SS scheme

DOI: 10.13009/EUCASS2022-6123

enhances the turbulence significantly by severely increasing the boundary layer thickness. However, also for the blowing on the PS scheme (shown in figure 3 b) the increase in *wake survey drag* and thus *inclusive drag* is apparent despite the fact, that Fahland *et al.* reported a reduction in *body drag*. What is interesting however is that this increase in *inclusive drag* does not correlate with an enhancement of the Re-Stress contribution in the drag assessment.

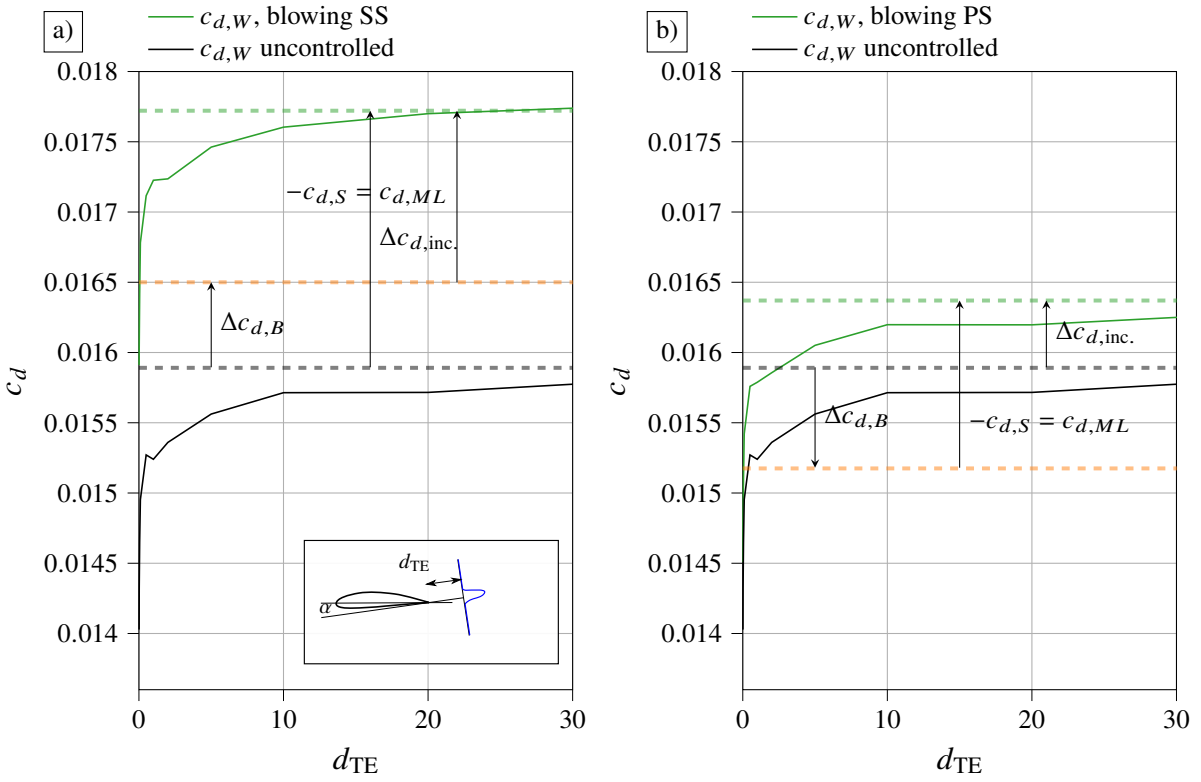

Figure 4: Relation of *wake survey* (solid lines) drag to *body drag* and derived *inclusive drag* (dashed lines) for different distance of the wake plane downstream of the trailing edge based on RANS data. NACA 4412, $Re = 4 \cdot 10^5$, $v_{\text{BLC}} = 0.1 U_\infty$

In a next step we take a look at the correlation of the *body drag* with the *wake survey drag* in figure 4. The assumptions for the *wake survey drag* include the flux leaving the control volume through the top and bottom boundary having a velocity equal U_∞ (figure 1). However this is not exactly true, because the velocity to either side of the airfoil is not U_∞ for a considerable distance, theoretically infinity. Therefore we have to calibrate the corresponding error of the *wake survey drag* assessment for the general flow pattern, *i.e.* a certain angle of attack for a certain airfoil. We do this by deriving a correction term $\Delta c_{d,W,c}$ for the converged *wake survey drag* result which we find to exist for far distances from the airfoil trailing edge:

$$\Delta c_{d,W,c} = c_{d,B,\text{unc.}} - c_{d,W,\text{unc.}}(d_{TE} = 50c) = 0.001524. \tag{8}$$

In figure 4 we show all quantities derived from the *body drag* corrected by this value. Clearly, including the correction term both body-integral and wake-integral quantities show good agreement for both flow control schemes, despite their very different effect on the *body drag*. Also it is obvious that the *wake survey drag* indeed resembles the *inclusive drag* well. This means the information of the penalty term $c_{d,S}$ of the considered flow control scheme on the *body drag* due to getting fluid elsewhere is present in such an experiment or simulation even if this origin is not considered directly in the setup.

This leads the investigation to the question of the development of *body drag* and *inclusive drag* (*wake survey drag* respectively) with increasing the flow rate of the BLC depicted in figure 5. As can be seen for the blowing on the SS case (figure 5 a)) the reduction in *friction drag* cannot even compensate the increase in *pressure drag* thus a strong increase in *body drag* is observable. This is accompanied by strong flow separations on the SS of the airfoil which also prevents the simulations to converge as well as the others. The *inclusive drag* (*wake survey drag* respectively) increases even stronger of course for the aforementioned reasons of BLC provision.

DOI: 10.13009/EUCASS2022-6123

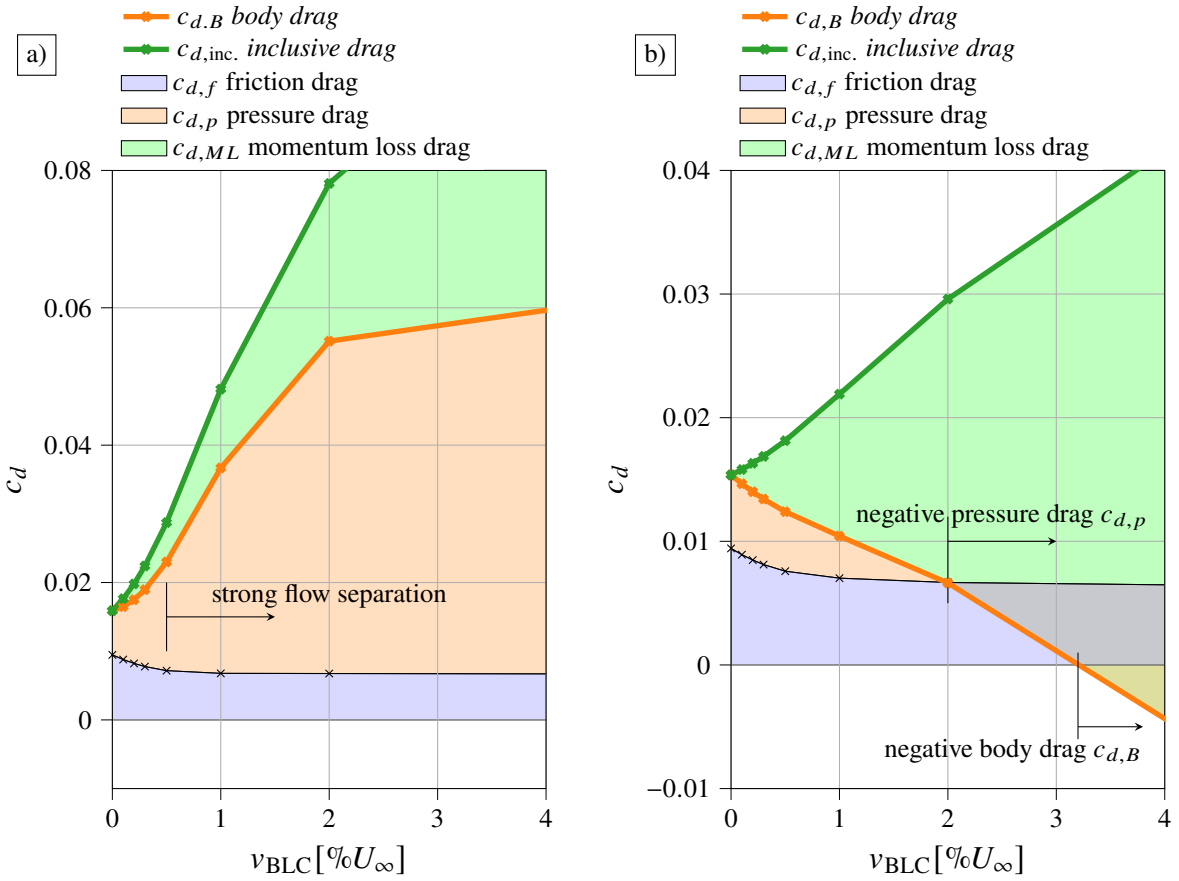

Figure 5: Drag portion development for increasing uniform blowing on PS intensity for NACA 4412, $Re = 4 \cdot 10^5$, $\alpha = 5°$ based on RANS data.

In case of blowing on the PS (figure 5b) of the airfoil the reduction in *friction drag* as accompanied by a reduction in *pressure drag* which leads to a decline in *body drag* with increasing BLC flow rate. The decrease in *body drag* is almost linear leading to a point where the *pressure drag* becomes negative and for higher BLC rate even the *body drag* gets negative. Clearly, the linearity resembles the proportionality of the source thrust term in equation 3 which is in fact acting like a source in a potential flow field, which also experiences thrust proportional to its strength. However, it becomes clear that the cost of such a *body drag* decrease is high when considering the *inclusive drag*. For the scheme shown here it is obvious that it cannot provide any *net drag* reduction if it is to be provided from the free-stream which requires the *inclusive drag* for proper drag assessment. Yet, this does not mean that it cannot be efficient because if this scheme is not provided by the free-stream but another suction BLC which already realises the sink drag effect, the *body drag* becomes the relevant figure of merit for drag assessment which shows a considerable drag reduction (figure 5b).

Our investigations show the importance of the correct drag quantity choice when judging the performance of an active flow control scheme, in our case uniform blowing or micro-blowing respectively. Moreover, it has been clarified that the corresponding distinctions are crucial also for the correct interpretation of drag measurement results in experimental investigations.

DOI: 10.13009/EUCASS2022-6123

4 Outlook on Experimental campaign

4.1 Measurement goals

For the experimental campaign we have several goals. Naturally, the original desire for an experimental campaign arose from demonstrating the validity of the numerical results of the large parametric study of Fahland *et al.* [6] which showed large performance enhancement capabilities for certain parameter combinations of uniform blowing on the pressure side of NACA 4-digit series airfoils. During the preparation for this campaign the literature review revealed the aforementioned disagreement in drag estimates of some numerical and experimental campaigns which led to our findings regarding the drag assessment and support system drag penalties which we now want to justify their significance using our experiment as well. Lastly we aim at closing the gap of possible porosities of the control surface which we found to exist after reviewing previous experimental studies. Figure 6 shows the wall-normal velocity in terms of dimensionless $C_q = v_{\mathrm{BLC}}/U_\infty$ over different levels of porosity.

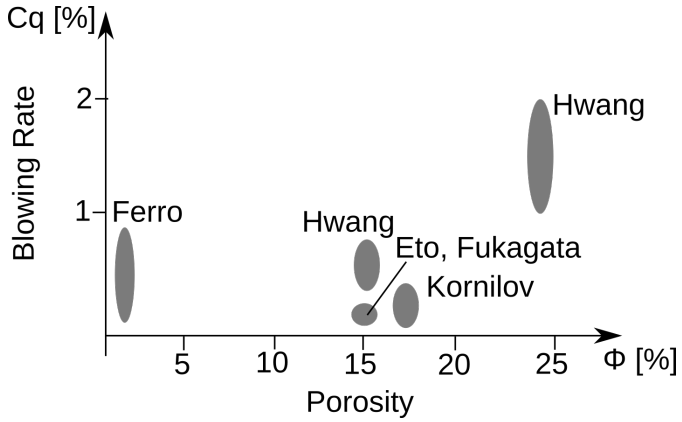

Figure 6: Literature data of micro-blowing experiments so far by Ferro [7], Hwang [9], Eto & Fukagata [5] and Kornilov [15, 14]

4.2 General Setup

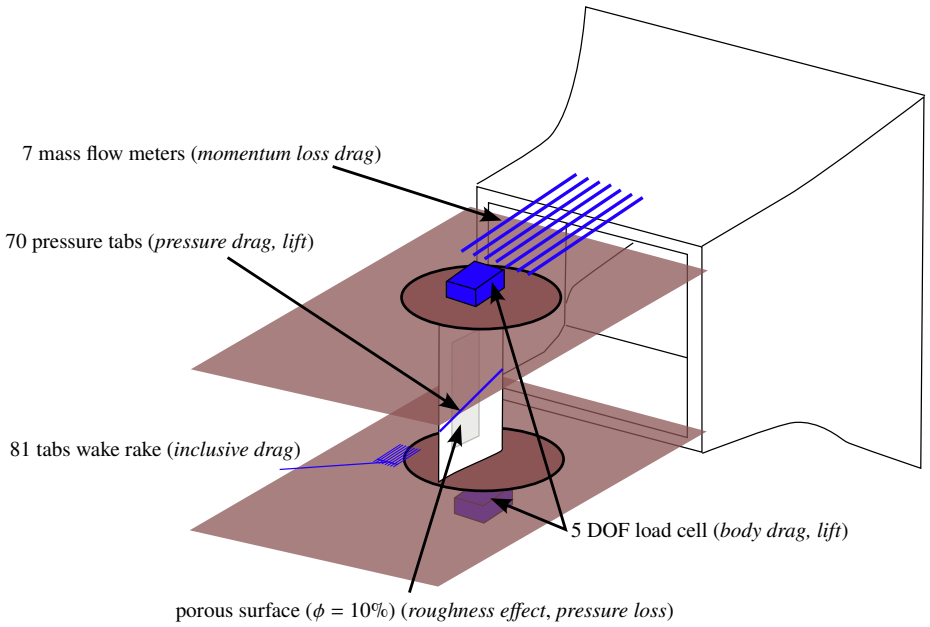

Figure 7: Schematic of general setup

The general setup for the intended experiments has been completed and is in validation testing with the HGR-

DOI: 10.13009/EUCASS2022-6123

airfoil [25]. It fields an open jet wind tunnel with extended side-plates in order to ensure two-dimensional flow. The boundary layer of the site plates starts at the wind tunnel nozzle with an elliptical leading edge of which the stagnation point position can be controlled via the bleed air flow. The measurement principles are depicted in figure 7. The specs of the complete setup including the custom airfoil wind-tunnel model will be as follows:

- Modified NACA 4412 airfoil
  - span $s = 1298mm$
  - chord $c = 750mm$
  - achievable chord Reynolds Number $Re_C \approx 2.9$Mio
  - 70 pressure tabs (MPS 4264 sensors)
  - smoothed pressure side TBL development compared to original NACA 4412
- Blowing Pressure Side TBL control scheme
  - laser-drilled thickness $d = 1mm$ Titanium sheet metal, 8Mio holes $d_H \approx 70\mu m$
  - span $s = 871mm$
  - chord $c = 351mm$
  - porosity $\phi = 10.06\%$
  - 7 individually controllable chambers
  - flow rate up to $c_q = 0.5\%$ for $U_\infty = 40m/S$
- Load cells
  - decoupled axes, air bearing
  - ME-Systeme KD40s Sensors, spanning 5N to 1kN nominal load
- Wake Rake
  - 81 tabs for total pressure
  - 8 tabs for static pressure
  - MPS4264 Sensors
- Flow meter
  - 7 testo hot film mass flow meter
  - 7 pressure drop flow meter over porous surface

As can be seen in figure 6 there is a gap of experimental investigations for porosity lower than $\phi_O = 15\%$. Hwang stated [9] that his experiments showed that this region could be interesting regarding the conflict of surface roughness induced by the porosity vs. the non-uniformity of the injected mass flux due to the finite character of the open area. This motivated us to choose the porosity of $\phi = 10\%$ for our experiments.

Intentionally every integral quantity has two means of measuring in our setup. For one, this way we want to make sure to have a more robust error estimate compared to using a single measurement principle. Furthermore we want to demonstrate in practice the drag relations we have shown in the present contribution numerically. Additionally we plan on doing PIV or StereoPIV measurements synchronized to the setup of figure 7 in order to correlate localized turbulent effects with integral quantities.

References

[1] M. Atzori, R. Vinuesa, G. Fahland, A. Stroh, D. Gatti, B. Frohnapfel, and P. Schlatter. Aerodynamic Effects of Uniform Blowing and Suction on a NACA4412 Airfoil. *Flow Turbulence Combust*, 105:735–759, April 2020.

[2] N. Beck, T. Landa, A. Seitz, L. Boermans, Y. Liu, and R. Radespiel. Drag Reduction by Laminar Flow Control. *Energies*, 11(1):252, January 2018.

[3] A. Betz. Ein Verfahren zur direkten Ermittlung des Profilwiderstandes. *ZFM*, 16:42–44, 1925.

[4] K. Eto, Y. Kondo, K. Fukagata, and N. Tokugawa. Friction Drag Reduction on a Clark-Y Airfoil Using Uniform Blowing. In *2018 Flow Control Conference*, Atlanta, Georgia, June 2018. American Institute of Aeronautics and Astronautics.

DOI: 10.13009/EUCASS2022-6123

[5] Kaoruko Eto, Yusuke Kondo, Koji Fukagata, and Naoko Tokugawa. Assessment of Friction Drag Reduction on a Clark-Y Airfoil by Uniform Blowing. *AIAA Journal*, 57(7):2774–2782, July 2019.

[6] G. Fahland, A. Stroh, B. Frohnapfel, M. Atzori, R. Vinuesa, P. Schlatter, and D. Gatti. Investigation of Blowing and Suction for Turbulent Flow Control on Airfoils. *AIAA Journal*, 59(11):4422–4436, July 2021.

[7] M. Ferro. *Experimental study on turbulent boundary-layer flows with wall transpiration*. PhD thesis, KTH Royal Institute of Technology, Stockholm, 2017. ISBN: 9789177295563 OCLC: 1023294987.

[8] B.A. Gregory, W.S. Walker, and A.N. Devereux. Wind-Tunnel Tests on the 30 per cent Symmetrical Griffith Aerofoil with Distributed Suction over the Nose. A.R.C. Technical Report 2647, Ministry of Supply, London, 1953.

[9] D. Hwang. Review of research into the concept of the microblowing technique for turbulent skin friction reduction. *Progress in Aerospace Sciences*, 40(8):559–575, November 2004.

[10] B. M. Jones. The measurement of profile drag by the pitot traverse method. Technical Report 1688, Cambridge, 1937.

[11] Y. Kametani and K. Fukagata. Direct numerical simulation of spatially developing turbulent boundary layers with uniform blowing or suction. *J. Fluid Mech.*, 681:154–172, August 2011.

[12] Y. Kametani, K. Fukagata, R. Örlü, and P. Schlatter. Drag reduction in spatially developing turbulent boundary layers by spatially intermittent blowing at constant mass-flux. *Journal of Turbulence*, 17(10):913–929, October 2016.

[13] R. B. Kinney. Skin-friction drag of a constant-property turbulent boundary layer with uniform injection. *AIAA Journal*, 5(4):624–630, April 1967.

[14] V. Kornilov. Combined Blowing/Suction Flow Control on Low-Speed Airfoils. *Flow Turbulence Combust*, 106(1):81–108, August 2020.

[15] V. I. Kornilov and A. V. Boiko. Efficiency of Air Microblowing Through Microperforated Wall for Flat Plate Drag Reduction. *AIAA Journal*, 50(3):724–732, March 2012.

[16] K.S.G. Krishnan, O. Bertram, and O. Seibel. Review of hybrid laminar flow control systems. *Progress in Aerospace Sciences*, 93:24–52, August 2017.

[17] B. Norton. *STOL progenitors: the technology path to a large STOL transport and the C-17A*. American Institute of Aeronautics and Astronautics, Inc, Reston, Va, 2002.

[18] C. L. Rumsey and T. Nishino. Numerical study comparing RANS and LES approaches on a circulation control airfoil. *International Journal of Heat and Fluid Flow*, 32(5):847–864, October 2011.

[19] Hermann Schlichting and K. Gersten. *Boundary-layer theory*. Springer, Berlin ; New York, 8th rev. and enl. ed edition, 2000.

[20] G. H. Schrauf and H. von Geyr. Simplified Hybrid Laminar Flow Control for the A320 Fin - Aerodynamic and System Design, First Results. In *AIAA Scitech 2020 Forum*, Orlando, FL, January 2020. American Institute of Aeronautics and Astronautics.

[21] A. Stroh. *Reactive Control of Turbulent Wall-Bounded Flows for Skin Friction Drag Reduction*. Dissertation, Karlsruhe Institute of Technology, Karlsruhe, 2016.

[22] A. Stroh, Y. Hasegawa, P. Schlatter, and B. Frohnapfel. Global effect of local skin friction drag reduction in spatially developing turbulent boundary layer. *J. Fluid Mech.*, 805:303–321, October 2016.

[23] U.H. von Glahn. Use of the Coanda Effect for obtaining Jet Feflection and Lift with a single Flat-Plate Deflection Surface. Technical Note 4272, NACA, Cleveland, Ohio, 1958.

[24] M. J. Walsh. Riblets for aircraft skin-friction reduction. *Langley Symposium on Aerodynamics*, 1:557–571, December 1986.

[25] R. Wokoeck, A. Grote, N. Krimmelbein, J. Ortmanns, R. Radespiel, and A. Krumbein. RANS Simulation and Experiments on the Stall Behaviour of a Tailplane Airfoil. In Ernst Heinrich Hirschel, W. Schröder, Kozo Fujii, Werner Haase, Bram Leer, Michael A. Leschziner, Maurizio Pandolfi, Jacques Periaux, Arthur Rizzi, Bernard Roux, Hans-Josef Rath, Carsten Holze, Hans-Joachim Heinemann, Rolf Henke, and Heinz Hönlinger, editors, *New Results in Numerical and Experimental Fluid Mechanics V*, volume 92, pages 208–216. Springer Berlin Heidelberg, Berlin, Heidelberg, 2006. Series Title: Notes on Numerical Fluid Mechanics and Multidisciplinary Design (NNFM).